MAPK signaling to the early secretory pathway revealed by kinase/phosphatase functional screening

Hesso Farhan,[1] Markus W. Wendeler,[1] Sandra Mitrovic,[1] Eugenio Fava,[2] Yael Silberberg,[4] Roded Sharan,[4] Marino Zerial,[3] and Hans-Peter Hauri[1]

[1]Biozentrum, Universität Basel, 4056 Basel, Switzerland
[2]High-Throughput Technology Development Studio, [3]Max Planck Institute of Molecular Cell Biology and Genetics, 01307 Dresden, Germany
[4]The Blavatnik School of Computer Science, Tel Aviv University, 69978 Tel Aviv, Israel

To what extent the secretory pathway is regulated by cellular signaling is unknown. In this study, we used RNA interference to explore the function of human kinases and phosphatases in controlling the organization of and trafficking within the secretory pathway. We identified 122 kinases/phosphatases that affect endoplasmic reticulum (ER) export, ER exit sites (ERESs), and/or the Golgi apparatus. Numerous kinases/phosphatases regulate the number of ERESs and ER to Golgi protein trafficking. Among the pathways identified, the Raf–MEK (MAPK/ERK [extracellular signal-regulated kinase] kinase)–ERK cascade, including its regulatory proteins CNK1 (connector enhancer of the kinase suppressor of Ras-1) and neurofibromin, controls the number of ERESs via ERK2, which targets Sec16, a key regulator of ERESs and COPII (coat protein II) vesicle biogenesis. Our analysis reveals an unanticipated complexity of kinase/phosphatase-mediated regulation of the secretory pathway, uncovering a link between growth factor signaling and ER export.

Introduction

The secretory pathway is permanently challenged by large amounts of newly synthesized proteins and lipids that need to be correctly sorted and transported. The first transport step is initiated by the incorporation of secretory proteins into COPII (coat protein II)-coated vesicles budding from the ER (Bonifacino and Glick, 2004; Lee et al., 2004). COPII coat assembly starts by activation of the small GTPase Sar1 by its exchange factor Sec12. Active Sar1 on ER membranes mediates the recruitment of the COPII subunits Sec23-Sec24 and Sec31-Sec13, which induces COPII vesicle budding. In mammalian cells, COPII vesicles form at ribosome-free transitional elements of the rough ER, termed ER exit sites (ERESs; Orci et al., 1991; Zeuschner et al., 2006). Thus, COPII proteins are faithful markers for ERESs. Sec16 also localizes to ERESs and plays a central role in the organization of ERESs and COPII vesicle biogenesis (Supek et al., 2002; Watson et al., 2006; Bhattacharyya and Glick, 2007; Iinuma et al., 2007; Farhan et al., 2008).

In mammals, COPII vesicles mediate cargo transport to the ER–Golgi intermediate compartment (ERGIC), where decisions are made either to recycle proteins back to the ER via COPI vesicles or to transport them on to the Golgi (Appenzeller-Herzog and Hauri, 2006). Retrograde transport from Golgi to ER is also mediated by COPI vesicles (Letourneur et al., 1994) and involves passage through the ERGIC, at least partially. Thus, the ERGIC is an intermediary station in bidirectional ER–Golgi trafficking.

In contrast to the advanced knowledge of the mechanisms underlying vesicular trafficking, it remains largely unknown to what extent the secretory pathway is regulated by cellular signaling pathways. A limited number of kinases and phosphatases have been implicated in the regulation of the early secretory pathway

Correspondence to Hans-Peter Hauri: Hans-Peter.Hauri@unibas.ch

E. Fava's present address is German Center for Neurodegenerative Diseases, D-53175 Bonn, Germany.

Abbreviations used in this paper: CNK1, connector enhancer of the kinase suppressor of Ras-1; ERES, ER exit site; ERGIC, ER–Golgi intermediate compartment; ERK, extracellular signal-regulated kinase; GO, Gene Ontology; LTK, leukocyte Tyr kinase; MEK, MAPK/ERK kinase; NF1, neurofibromin 1; SLE, systemic lupus erythematosus.

The Rockefeller University Press $30.00
J. Cell Biol. Vol. 189 No. 6 997–1011
www.jcb.org/cgi/doi/10.1083/jcb.200912082

(Kapetanovich et al., 2005; Palmer et al., 2005; Bejarano et al., 2006), but detailed understanding of the high-order regulation calls for a systematic approach.

Results

Kinases and phosphatases regulating the early secretory pathway

To identify genes regulating the ER–Golgi system, we used an siRNA-based knockdown approach targeting all human kinases and phosphatases for effects on the localization of ERGIC-53, a sensitive marker for changes in trafficking and morphology of the early secretory pathway (Schweizer et al., 1988; Klumperman et al., 1998). The screen was performed in HeLa cells stably expressing GFP-tagged ERGIC-53 (Ben-Tekaya et al., 2005). Because of its cycling, the type I transmembrane protein ERGIC-53 is a sensitive indicator for both changes in bidirectional traffic in the secretory pathway and organelle integrity.

Cells were transfected with three siRNAs (not pooled) to each of the 916 known and putative protein and lipid kinases and phosphatases (724 kinases; 192 phosphatases; Table S1). Transfection efficiency was >80% on average, and down-regulation was >70% when tested on various selected proteins. All siRNAs had nonoverlapping sequences. 48 h after transfection, cells were fixed and stained with DAPI/Syto42 to label nuclei and cytoplasm, providing information on cell number. Images were acquired by automated spinning disk confocal microscopy. 16 frames/well were acquired for each GFP–ERGIC-53 and DAPI/Syto42. Images were analyzed visually. Kinases/phosphatases were chosen for further analysis if two out of three siRNAs affected the pattern of ERGIC-53. Kinases/phosphatases were excluded if silencing either compromised cell viability (i.e., strong reduction in cell number) or had previously been reported to induce apoptosis in an siRNA screen in HeLa cells (MacKeigan et al., 2005).

Our primary screen retrieved 154 kinases/phosphatases hits. To validate them in a secondary screen, endogenous ERGIC-53 was covisualized with markers for ERESs (Sec31) and Golgi (giantin) by double immunofluorescence microscopy. 122 of the original 154 hits were validated as true positive (~79%; Table S2), of which ~12% were phosphatases. 56% belonged to one of the eight kinase classes (Fig. 1 A). The remainder (~32%) belonged to the group of atypical, putative, or uncharacterized kinases and regulatory subunits. Overall, ~8% (16 out of 193) of the phosphatome library and ~15% (106 out of 723) of the kinome library were true hits. Importantly, based on screening various databases and the literature, we conclude that at least 118 out of the 122 identified kinases and phosphatases are expressed in HeLa cells (Table S2).

Hits were phenotypically grouped (Fig. 1 B). The ER class comprises all hits with enhanced ER staining of ERGIC-53 and with reduction of peripheral ERGIC clusters (Fig. 1, compare C with D; and Table S2). ERES number was reduced, but the Golgi was unchanged. The Golgi class comprises all hits with fragmented or tubulated Golgi. Peripheral ERGIC clusters and ERESs were unaffected, but juxtanuclear ERGIC was lost (Fig. 1 F and Table S2). The overall microtubule organization was unaffected (Table S2). The mixed class includes all kinases/phosphatases that did not fit into the ER or Golgi class. Our screen retrieved the known kinase regulators of intracellular trafficking, PCTAIRE1/PCTK1, MST4, PIK4CA, and SCYL1. Silencing PCTAIRE1/PCTK1 reduces the number of ERESs (Palmer et al., 2005), which is consistent with our finding that PCTK1 is an ER-class hit exhibiting a reduced number of peripheral ERGIC punctae (Table S2) and ERESs. Silencing MST4 disrupts Golgi morphology (Preisinger et al., 2004). In our screen, we identified MST4 as a Golgi-class hit with fragmented Golgi (Table S2). We previously showed that a knockdown of PIK4CA (PI4-kinase IIIα) affects ERES number and ERES adaptation to cargo load (Farhan et al., 2008). In the current screen, PIK4CA was identified as a mixed-class hit with a reduced number of peripheral ERGIC punctae (Table S2) and slight fragmentation of the Golgi (not depicted). Finally, SCYL1 has been shown to bind COPI and to be involved in retrograde Golgi to ER transport (Burman et al., 2008). In the current work, SCYL1 appeared as a mixed-class hit that reduced the number of peripheral ERGIC punctae (Table S2) and tubulated the Golgi (Fig. 1 E). Thus, besides the few known kinases, our screen identified a large number of novel potential regulators of the early secretory pathway.

Functional predictions from network analysis

ER- and Golgi-class hits were assembled into a network using the STRING database (http://string.embl.de/; Jensen et al., 2009). ER-class hits were well connected (Fig. 2 A), whereas Golgi-class hits were not (Fig. 2 B). The connectivity of ER-class hits enabled us to perform functional annotation clustering using the DAVID database (http://david.abcc.ncifcrf.gov/; Huang et al., 2009). We searched for specific enrichment of our hits within signaling pathways. ER-class hits were associated with 13 different pathways. Nine ER-class hits were annotated to the MAPK pathway (Fig. 2 C). The mitogenic and the stress signaling pathways involving MAPKs are illustrated in Fig. S1 A. Interestingly, the mitogenic MAPK signaling pathway only included ER-class hits. Lipid kinases were over-represented (26% of the lipid kinome vs. 14% of the protein kinome), which is consistent with the fact that we are studying membrane trafficking. The phosphatidylinositol and inositol phosphate metabolism was specifically associated with ER- and mixed-class hits (Fig. 2 C and Fig. S1 B). This is consistent with the notion that phosphatidylinositol-modifying kinases may play a role in ER export (Blumental-Perry et al., 2006; Farhan et al., 2008).

We also wondered whether our collection of Golgi-class hits contains signatures of signaling pathways or cellular processes. This issue cannot be addressed with the same approach used for the analysis of the ER-class hits because Golgi-class hits are associated with only one signaling pathway (Fig. 2 C). This difference is explainable by poor hit connectivity, which does not allow functional annotation clustering using the DAVID database (Fig. 2 B) and thus calls for an alternative approach. We used a recently described new way of anchored network construction (Yosef et al., 2009). The rationale of this approach is to anchor the Golgi-class hits to known proteins involved in Golgi structure and biology. We used several anchor proteins. The Golgi matrix protein GM130 (GOLGA2) was chosen because of its well

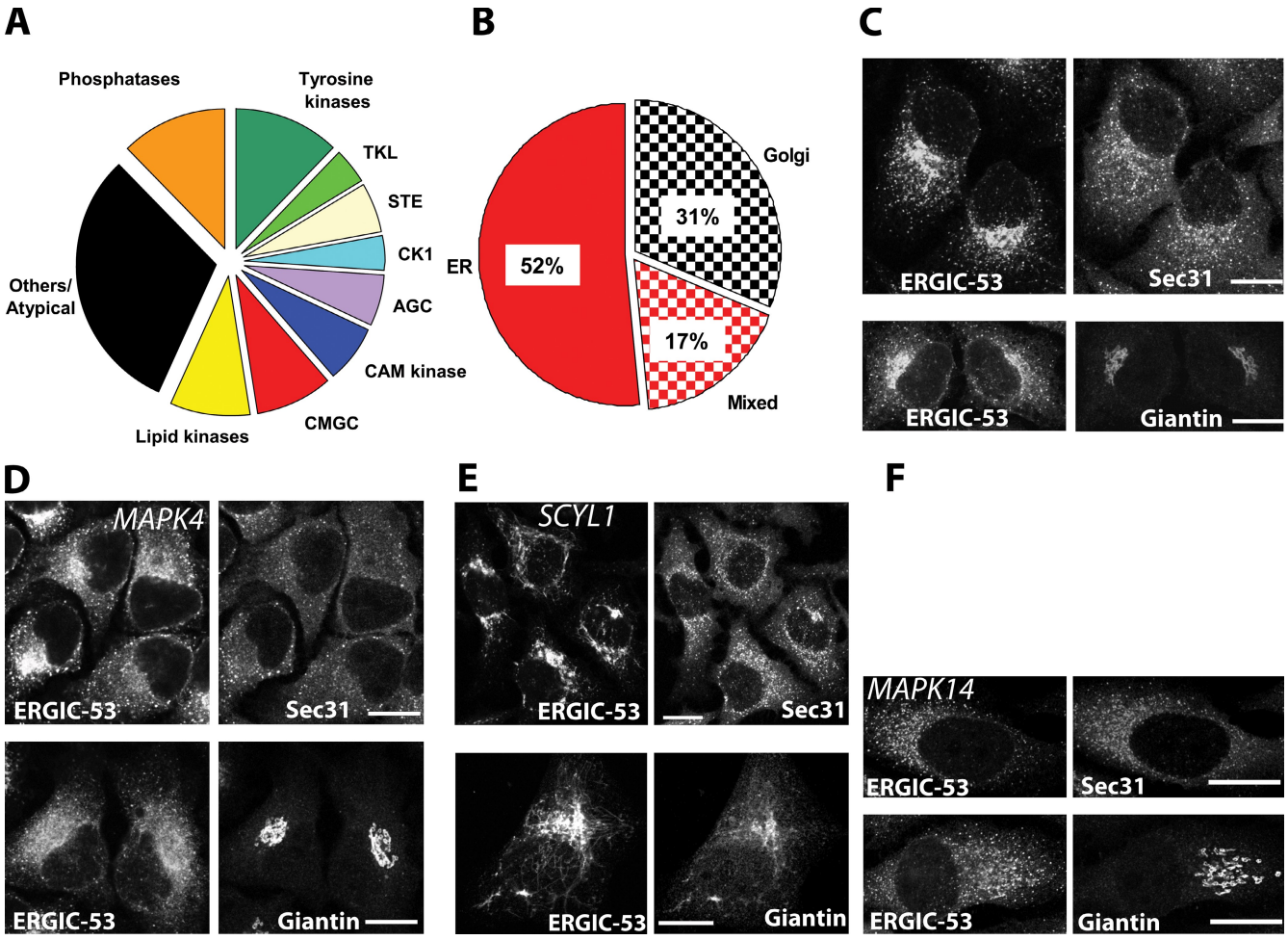

Figure 1. **Classification of kinase/phosphatase hits.** (A) Assignment to protein families. TKL, Tyr kinase–like; STE, related to sterile kinases; CK1, casein kinase 1; AGC, kinase family containing PKA, PKG, and PKC; CAM kinase, calmodulin kinases; CMGC, kinase family containing CDK, MAPK, GSK, and CKL. (B) Phenotypic classification of hits. (C–F) Immunofluorescence of phenotypes. HeLa cells transfected with control siRNA (C) or siRNA to MAPK4 (example of the ER class; D), SCYL1 (example for the mixed class; E), and MAPK14 (example for the Golgi class; F) are shown. Cells were fixed 72 h after transfection and double stained with antibodies against the indicated proteins. Bars, 10 µm.

accepted role in Golgi structural maintenance. Moreover, GM130 was shown to interact with the Golgi-class hit MST4 (Preisinger et al., 2004). We also used the cargo receptor p24-α (TMED2) and the GTPase Arf1. Both proteins play important roles in Golgi biology and bidirectional ER to Golgi trafficking. Because the Golgi is known to play an important role in cell polarity, we constructed a multianchored network with the known polarity regulators Par3 (PARD3), Par6 (PARD6A), PKC-ζ (PRKCZ), Scrib, Pals1 (MPP5), and Cdc42 (Fig. 3 A). Four networks were established, each of which connected all Golgi-class hits. The four networks were then merged by generating a union using the Cytoscape software and analyzed using the BiNGO plugin (Fig. 3 A). BiNGO detects specific enrichment of Gene Ontology (GO) annotations for cellular processes. To test for the enrichment of signaling pathways, we analyzed the merged network using the DAVID database. Several signaling pathways and cellular processes were enriched (Fig. S1 C). By combining the BiNGO and DAVID analyses, we note possible links between Golgi structure and apoptosis, proliferation, cell size, and infection. Golgi positioning was previously shown to also play an important role in directional cell migration (Yadav et al., 2009). However, the focus of previous studies was on structural proteins of the Golgi (Rivero et al., 2009; Yadav et al., 2009). We asked whether Golgi-class hits regulate cell migration. Indeed, in a scratch wound assay, the knockdown of various Golgi-class members impaired correct position of the Golgi and wound healing (Fig. 4). Thus, besides revealing signaling pathways associated with ER hits, our study provides a resource of signaling molecules that regulate Golgi shape and thereby cell migration.

The MAPK pathway regulates ERESs and ER exit

Because numerous ER-class hits are members of the MAPK pathway, we asked whether the MAPK pathway affects ERESs. To determine the range within which ERESs can be regulated in our experimental systems, we silenced Sec16, a key regulator of ERESs. Knockdown of Sec16 maximally reduces ERES number by 50% (Fig. 5 A; Farhan et al., 2008). If the MAPK pathway regulates ERESs, its hyperactivation should increase, whereas its inhibition should decrease ERES number. This was indeed observed. Silencing NF1 (neurofibromin 1), which hyperactivates the MAPK pathway (Fig. S2 A), increased the number of ERESs

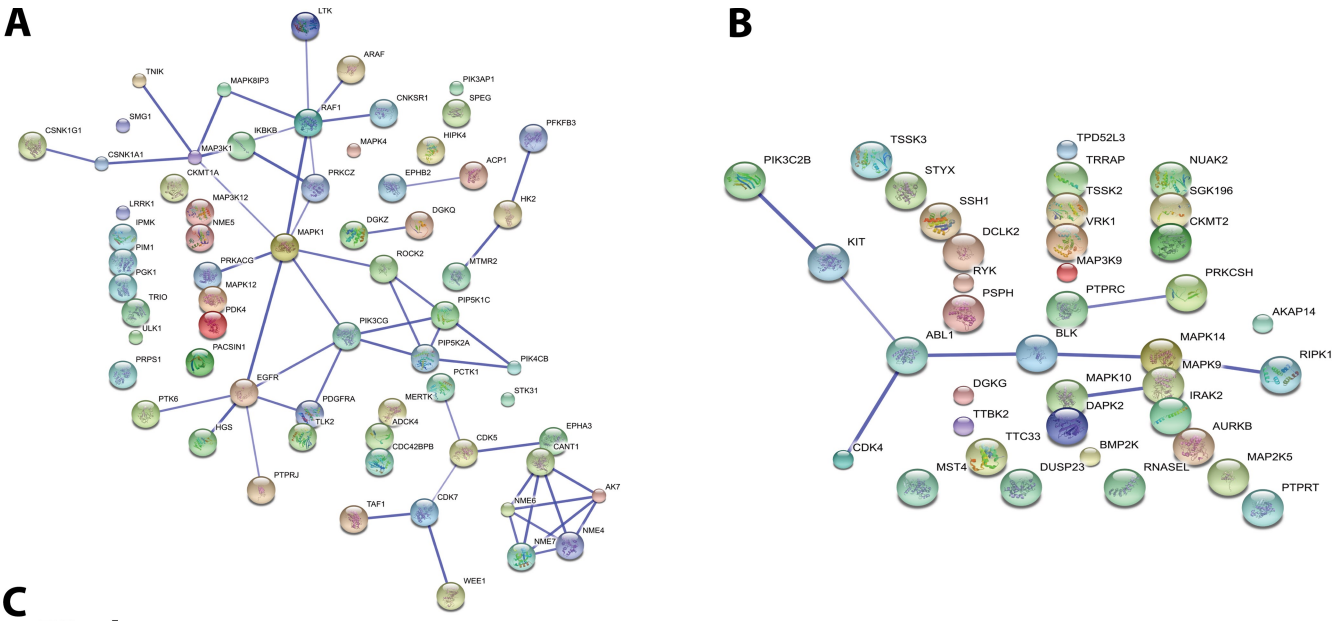

C ER-class

KEGG pathway	P-value	Genes
hsa05221:Acute myeloid leukemia	1.65E-04	ARaf1, Pim1, MAPK1, IKBKB, PIK3CG, Raf1
hsa04070:Phosphatidylinositol signaling system	7.54E-04	PIP5K2A, DGKZ, PIP5K1C, PIK3CG, PIK4CB, DGKQ
hsa00562:Inositol phosphate metabolism	0.001386	PIP5K2A, IPMK, PIP5K1C, PIK3CG, PIK4CB
hsa05215:Prostate cancer	0.001395	ARaf1, PDGFRA, MAPK1, IKBKB, PIK3CG, Raf1
hsa04910:Insulin signaling pathway	0.001662	PRKCZ, ARaf1, MAPK1, IKBKB, PIK3CG, Raf1, PRKACG
hsa05214:Glioma	0.002538	ARaf1, PDGFRA, MAPK1, PIK3CG, Raf1,
hsa04010:MAPK signaling pathway	0.002956	MAPK12, PDGFRA, MAPK1, IKBKB, Raf1, MAP3K1, PRKACG, MAPK8IP3, MAP3K12
hsa04810:Regulation of actin cytoskeleton	0.00405	PIP5K2A, ARaf1, PIP5K1C, PDGFRA, MAPK1, PIK3CG, Raf1, ROCK2
hsa05218:Melanoma	0.004225	ARaf1, PDGFRA, MAPK1, PIK3CG, Raf1
hsa05212:Pancreatic cancer	0.005173	ARaf1, MAPK1, IKBKB, PIK3CG, Raf1
hsa05220:Chronic myeloid leukemia	0.00543	ARaf1, MAPK1, IKBKB, PIK3CG, Raf1
hsa05210:Colorectal cancer	0.008848	ARaf1, PDGFRA, MAPK1, PIK3CG, Raf1
hsa04930:Type II diabetes mellitus	0.00914	PRKCZ, MAPK1, IKBKB, PIK3CG

Mixed-class

KEGG pathway	P-value	Genes
hsa00562:Inositol phosphate metabolism	3.40E-04	PIK4CA, INPP4B, SYNJ1, PIP5K2C
hsa04070:Phosphatidylinositol signaling system	1.10E-03	PIK4CA, INPP4B, SYNJ1, PIP5K2C

Golgi-class

KEGG pathway	P-value	Genes
hsa04620:Toll-like receptor signaling pathway	0.00507	MAPK9, MAPK10, RIPK1, MAPK14

Figure 2. **Network of kinase hits indicates a role for MAPK signaling in the regulation of ER export.** (A) All ER-class hits were assembled into a network using the STRING database. (B) Assembly of all of the Golgi-class hits into a network using the STRING database. Edges in both networks indicate an interaction that is experimentally verified or an association into a signaling pathway. (C) ER-, mixed-, and Golgi-class hits specifically enriched in signaling pathways deduced from the DAVID database.

by ~20% (Fig. 5 A). In contrast, silencing ERK2 (an ER-class hit) but not ERK1 significantly reduced the number of ERESs by ~30% (Fig. 5 A). Thus, the full range by which the MAPK pathway can regulate ERES number is ~50%. Knockdown of ERK2 did not affect the levels of ERK1 (Fig. 5 B), indicating that the effect of ERK2 silencing was specific. To further support this,

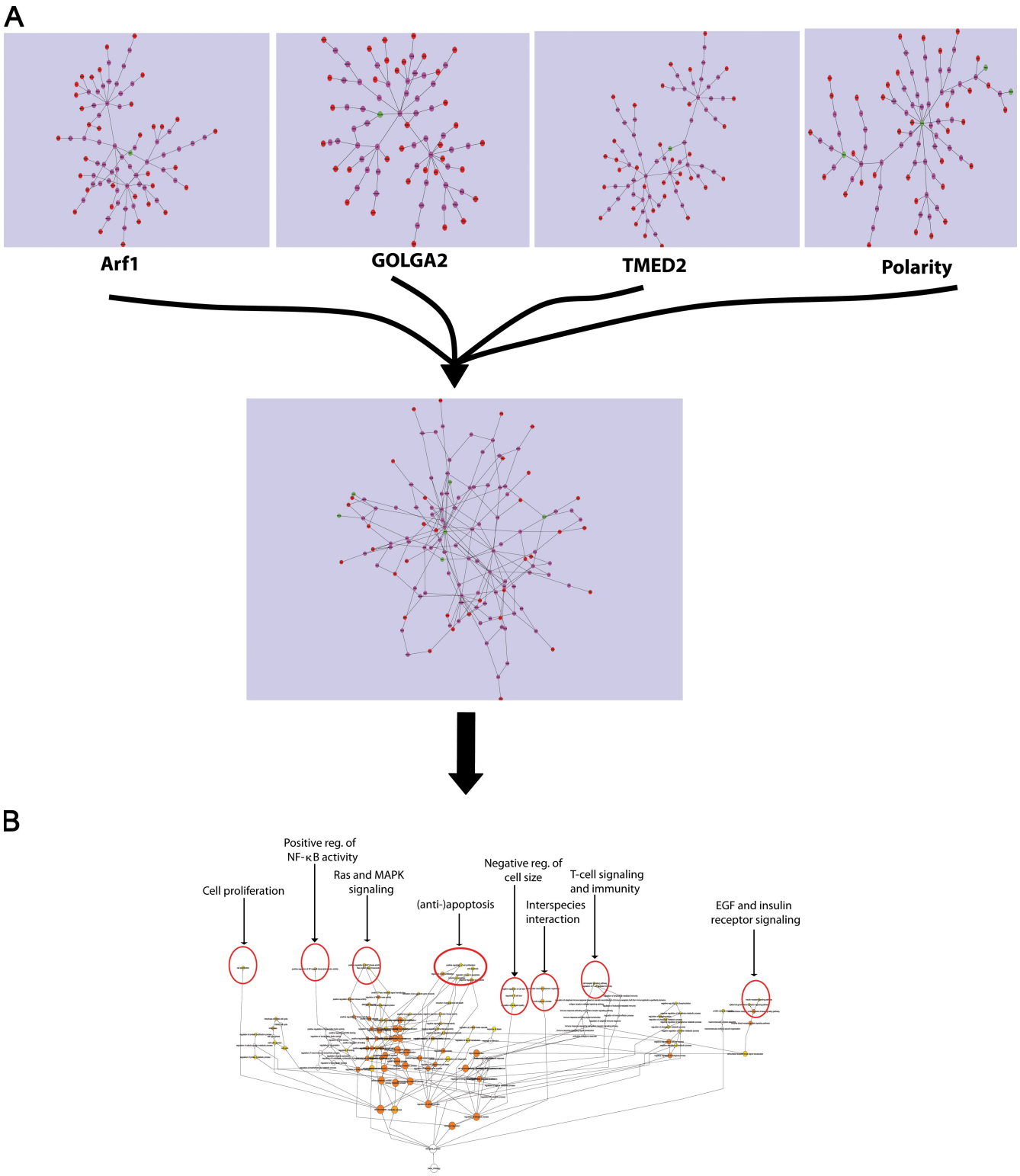

Figure 3. **BiNGO analysis of Golgi-class hits from four anchored networks.** (A) Four networks were generated with the Golgi-class hits anchored to GOLGA2, TMED2, ARF1, and polarity regulators (Par3, Par6, Cdc42, Pasl1, PKC-ζ, and Scrib). Networks were merged using the Cytoscape software and analyzed using the BiNGO 2.3 plugin. GO term cellular processes were scored at a significance value of at least 0.001. The Benjamini-Hochberg false discovery rate correction was used. (B) The network of cellular processes displayed in a hierarchical layout. Large PDF versions of these networks and their underlying data (which can be opened and visualized in Cytoscape) can be found in the online supplemental material.

we performed rescue experiments with Flag-tagged rat ERK2, which is not recognized by the siRNA to human ERK2. Cells were transfected with control or ERK2 siRNA and processed for ERES analysis 72 h later. In the rescue experiment, the Flag-tagged rat ERK2 cDNA was transfected 24 h before ERES analysis. Fig. 5 C shows that the Flag-tagged rat ERK2 can reincrease the number

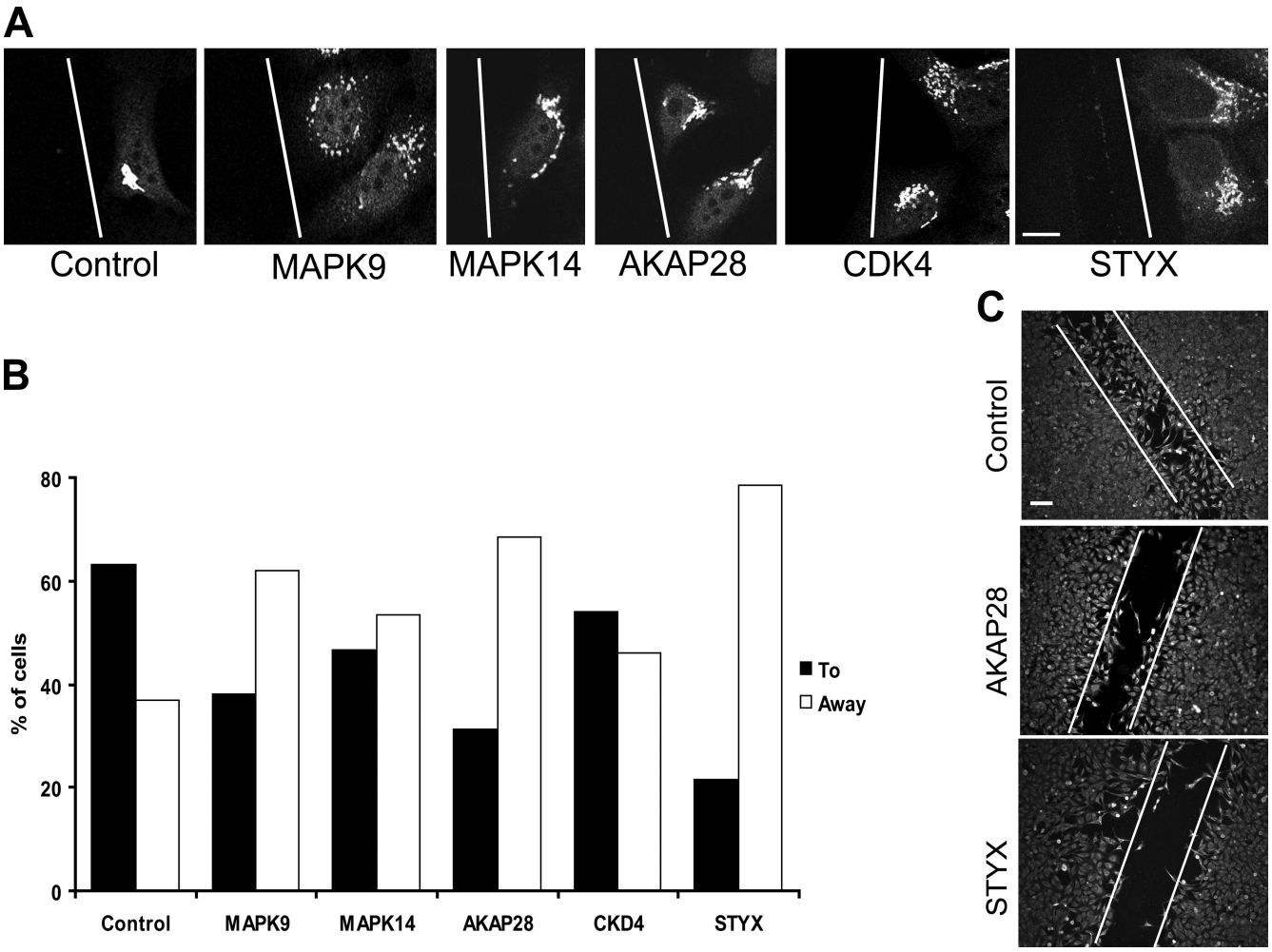

Figure 4. **Kinases and phosphatases of the Golgi class inhibit orientation of the Golgi toward a scratch wound.** HeLa cells were transfected with siRNAs to the indicated genes. After 72 h, a scratch wound was introduced. 6 h later, cells were fixed and stained for giantin to label the Golgi. (A) Representative images. (B) Quantification of two experiments with at least 35 cells each displayed as the percentage of cells exhibiting Golgi orientation to and away from the wound. (C) 48 h after the indicated knockdown, a wound was introduced, and cells were fixed 24 after later. Cells were labeled with FITC-tagged Con A. Note that STYX and AKAP28 knockdown cells fail to close the wound, in contrast to control cells. (A and C) White lines indicate the position of the scratch. Bars: (A) 10 µm; (C) 200 µm.

of ERESs, very much in contrast to a kinase-dead version of ERK2 (ERK2-K52R).

Next we tested whether the decrease in the number of ERESs translates into an effect on ER to Golgi transport. Silencing of ERK2 indeed reduced ER to Golgi transport of endogenous transferrin receptor in HeLa cells (Fig. 5 D). Because ERGIC-53 was used as a readout in our screen, we also tested transport of the ERGIC-53 cargo protein α1-antitrypsin. Inhibition of the MAPK pathway by PD98059 reduced transport of α1-antitrypsin (Fig. 5 E).

The MAPK pathway is regulated by scaffolds (Kolch, 2005). Our library included the CNK1 (connector enhancer of the kinase suppressor of Ras-1) and the kinase suppressor of Ras-1 and -2. In addition, MEKK1 is also thought to act as a scaffold (Karandikar et al., 2000). In our screen, CNK1 and MEKK1 were ER-class hits. Knockdown of CNK1 (Fig. 5 A) and MEKK1 (not depicted) reduced the number of ERESs. The effect of CNK1 was weak, but this was to be expected because CNK1 knockdown does not completely block the MAPK pathway but rather flattens the response curve to mitogens (Fig. S2 B). As expected for a scaffold, overexpression of HA-tagged CNK1 also had a negative effect and thus reduced ERES number (Fig. 5 A). Collectively, these results show that the Raf–MEK (MAPK/ERK [extracellular signal-regulated kinase] kinase)–ERK pathway, via ERK2, regulates the number of ERESs and ER to Golgi transport.

ERK2 stimulates COPII vesicle budding

Does ERK2 affect the biogenesis of transport vesicles? We used an established in vitro COPII vesicle budding assay to address this question (Kim et al., 2005). HeLa microsomes were incubated with ERK2-depleted HeLa cytosol, ATP-regenerating system, and GTP for 30 min at 25°C, and the appearance of ERGIC-53 in the vesicle fraction was monitored. The addition of purified ERK2 to the reaction mixture increased the amount of ERGIC-53 in the vesicle fraction (Fig. 6), indicating that ERK2 stimulates the formation of COPII vesicles at the ER. Our budding assay truly measures COPII vesicle production because depletion of Sec24A+B from the cytosol affected incorporation of

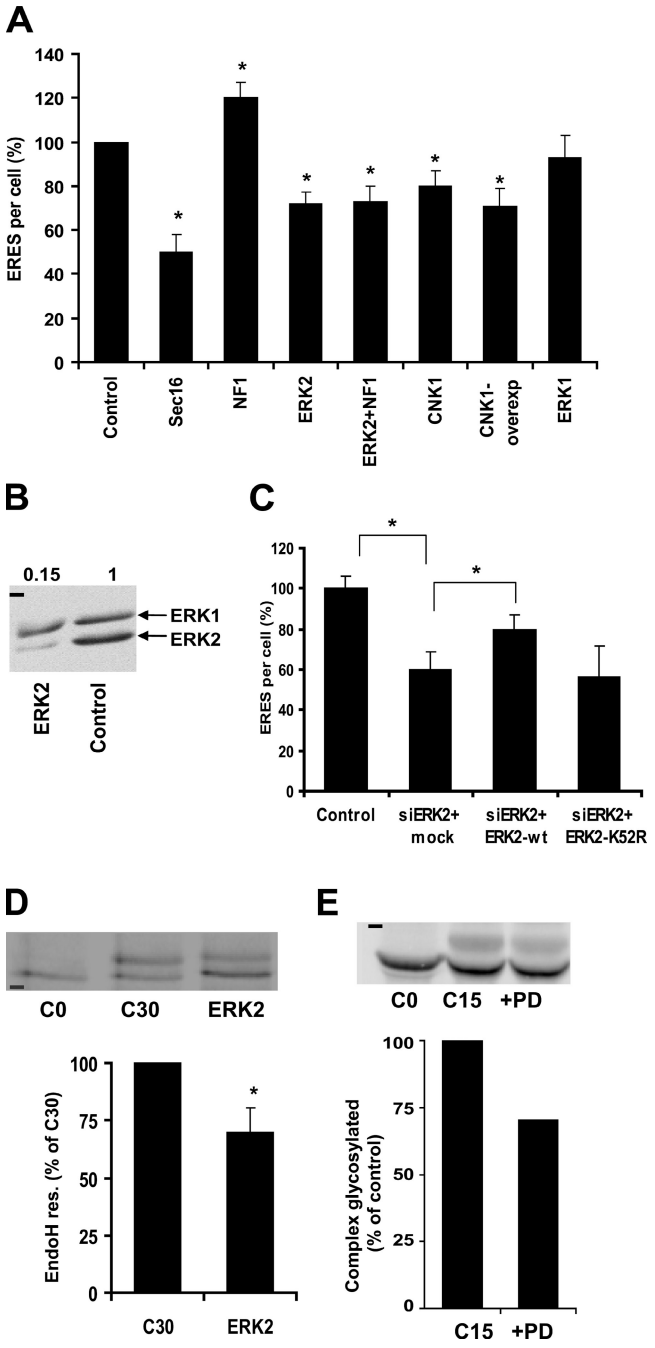

Figure 5. **A role for MAPK signaling in the regulation of ERES number and ER to Golgi transport.** (A) HeLa cells were transfected with the indicated siRNAs and fixed after 72 h. Anti-Sec31–labeled ERESs were quantified (means ± SD; $n = 3$). Asterisks indicate statistically significant differences (*, $P < 0.05$) from control (unpaired *t* test). (B) Cells were transfected with control or ERK2 siRNA. After 72 h, cells were lysed, and ERK1/2 was detected by immunoblotting. (C) HeLa cells were transfected with control or ERK2 siRNA (siERK2). After 48 h, the ERK2 siRNA–treated cells were left untreated (mock) or were transfected with Flag-tagged ERK2 cDNA or Flag-tagged ERK2-K52R cDNA. Cells were fixed 24 h later and stained for Flag and Sec31, and ERESs were counted. Asterisks indicate statistically significant differences (*, $P < 0.05$). (D) ER–Golgi transport of endogenous transferrin receptor was measured 72 h after transfection with the indicated siRNAs. Cells were subjected to pulse-chase experiments with [^{35}S]Met. Transferrin receptor was immunoprecipitated, treated with Endo H, separated by SDS-PAGE, and visualized by autoradiography. C0 and C30: control siRNA transfected and chased for 0 min and 30 min, respectively. ERK2: knockdown cells chased for 30 min. The bar diagram shows means ± SD ($n = 3$). The asterisk indicates statistically significant difference (*, $P < 0.05$) from control (unpaired *t* test). (E) ER–Golgi transport of endogenous α1-antitrypsin in HepG2 cells. 2 d after plating, cells were subjected to pulse-chase experiments with [^{35}S]Met. Cells were treated with DMSO (C) or the MEK inhibitor PD98059 (+PD) for 30 min before the pulse. Cells were pulsed for 10 min and chased for 15 min. C0 and C15: DMSO-treated cells chased for 0 min and 15 min, respectively. +PD: PD98059-treated cells chased for 15 min. The bar diagram is an evaluation of two independent experiments. (B, D, and E) The black lines on the blot indicate the position of the 50-kD (B and E) or 75-kD (D) molecular mass marker.

ERGIC-53 into vesicles (Fig. S3). We showed previously that ER export of ERGIC-53 is dependent on these Sec24 isoforms (Wendeler et al., 2007).

Sec16 is a target of the Raf-MEK-ERK signaling pathway

Sec16 is a key regulator of ERES biogenesis and maintenance, making it a prime candidate for an ERK2 target. We first assessed whether the MAPK pathway affects the in vivo dynamics of Sec16. This is best probed by FRAP of individual ERESs labeled by GFP-tagged Sec16. As shown in Fig. 7 A, GFP-Sec16 (National Center for Biotechnology Information Protein accession number O15027) nicely recovered after photobleaching of control cells as opposed to ERK2-silenced cells or cells in which the MAPK pathway was pharmacologically blocked. This is also illustrated by the significantly higher mobile fraction of Sec16 under control conditions (Fig. 7 B). In addition, we compared fluorescence recovery in serum-starved cells and cells treated with EGF (for 10 min). Treatment with EGF enhanced fluorescence recovery of Sec16 (Fig. 7 C) and increased the mobile fraction of Sec16 (Fig. 7 D). The change in mobility of Sec16 also translated into a change in the mobility of downstream COPII components. Treatment with EGF increased the recovery and mobile fraction of YFP-tagged Sec24D (Fig. 7, E and F). Because Sec16 responds to alterations of the MAPK pathway, it is a likely ERK2 target.

We monitored whether Sec16 is phosphorylated on a Ser/Thr-Pro sequence using a MAPK substrate antibody. This would be expected if Sec16 was an ERK target. GFP-Sec16 was immunoprecipitated, subjected to SDS-PAGE, and immunoblotted with antibodies to Sec16. The blots were stripped and reprobed with antibodies to a phosphorylated MAPK substrate. If Sec16 is phosphorylated on a MAPK target sequence, a band should appear at the same position as the Sec16 band before stripping. This was indeed observed. Fig. 8 A shows that Sec16 was phosphorylated on a MAPK target sequence, and this phosphorylation diminished when cells were cultured in the absence of mitogens (that is, in serum-free medium). Because Sec24D also responded to EGF treatment in our FRAP assay, we tested whether Sec24D is also recognized by the MAPK substrate antibody. However, this was not the case (unpublished data). This result indicates that the change in the mobility of Sec24D is not caused by phosphorylation by the MAPK pathway. Most likely, the increase of Sec24D mobility is indirectly induced by Sec16.

To more directly test whether Sec16 is phosphorylated by ERK, we performed in vitro experiments. Fig. 8 B shows that immunoisolated GFP-Sec16 from serum-starved cells, which are

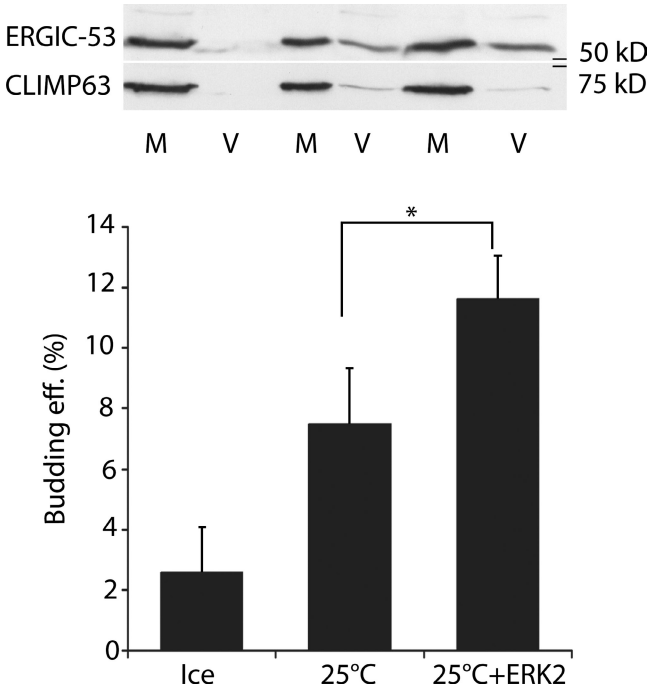

Figure 6. **ERK2 stimulates COPII vesicle budding.** HeLa microsomes were incubated for 30 min with ATP and an ATP-regenerating system, GTP, and cytosol of ERK2-silenced HeLa cells in the presence or absence of purified ERK2. COPII vesicles (V) were collected by centrifugation and immunoblotted for anti–ERGIC-53 and anti–CLIMP-63 (ER marker). The asterisk represents a statistically significant difference (*, $P < 0.05$; paired *t* test). Error bars indicate ±SD. M, 33% microsome input.

not phosphorylated, can be phosphorylated by incubation with immunoprecipitated active ERK (Fig. 8 B). To exclude that Sec16 was phosphorylated by a nonspecific component in the phospho-ERK immunoprecipitate, we performed experiments with recombinant ERK2. Recombinant active ERK2 also phosphorylated Sec16 (Fig. 8 C). Of note, both immunoprecipitated phospho-ERK and recombinant active ERK2 were active under our assay conditions as they were able to phosphorylate Elk1, a well known ERK target (Fig. 8 D).

In a next series of experiments, we attempted to identify the phosphorylation site or sites in Sec16 targeted by ERK2. A Sec16 mutant lacking the first 923 aa (Sec16-Δ923) still correctly localizes to ERESs (Bhattacharyya and Glick, 2007). This offers the possibility to test whether the phosphorylation site is located within the first 923 aa of Sec16. Sec16-Δ923 was not phosphorylated by ERK2 (Fig. 8 E) and, unlike wild-type Sec16, its mobility on ERESs did not respond to EGF treatment in the FRAP experiment (Fig. 8, E and F). This indicates that the phosphorylation site is likely located within the N-terminal 923 residues. Searching the amino acid sequence by Scansite (http://scansite.mit.edu/) revealed T415 as the most probable ERK target. We mutated T415 to Ile (Sec16-T415I), which reduced the ability of recombinant active ERK2 to phosphorylate Sec16 by at least 60% (Fig. 8 C), without affecting Sec16 localization (not depicted). The residual signal is most likely caused by minor phosphorylation of other residues by ERK2 in vitro (according to Scansite, there are 27 theoretical Pro-dependent Ser or Thr sites in Sec16, 14 of which are within the N-terminal 923 aa). This conclusion is supported by the finding that, at steady-state, Sec16-T415I exhibited some remaining phosphorylation (10–30% of Sec16-WT) when immunoprecipitated from HeLa cells (Fig. 8 H). Like Sec16-Δ923, Sec16-T415I did not respond to EGF treatment in the FRAP experiment (Fig. 8, I and J), supporting the notion that T415 is an important site for the regulation of Sec16 by ERK signaling.

Next, we asked whether the mutation of Thr415 to Ile affects the number of ERESs. To this end, we overexpressed either GFP-tagged wild-type Sec16 (Fig. 9 A) or GFP-tagged Sec16-T415I (Fig. 9 B). After 24 h, ERESs were stained for Sec31 and quantified. We also determined the effect of the mutation on peripheral ERGIC structures by staining for ERGIC-53. Exogenous expression of Sec16 exerts a negative effect on ERESs if the level of expression is too high. Therefore, we compared cells with only moderate GFP (i.e., Sec16) levels. In addition, we only compared cells with similar expression levels of GFP-Sec16 constructs. For quantification, we determined the value of GFP fluorescence and normalized it by the area. The mean fluorescence values (in arbitrary units) of cells expressing GFP–ERGIC-53 and GFP–Sec16-T415I were 3.48 ± 1.08 and 3.57 ± 1.46, respectively (means ± SD; three independent experiments). Expression of GFP–Sec16-T415I reduced the number of both ERESs and peripheral ERGIC punctae (Fig. 9 C). Furthermore, ERGIC-53 exhibited a stronger ER pattern in cells expressing the mutant Sec16, reminiscent of the ER-class hits (Fig. 9 B). The degree of down-regulation of ERESs was comparable with that observed in ERK2 knockdown cells (Fig. 5 A).

If Sec16 is a target of the MAPK pathway, its hyperactivation should increase the level of Sec16 phosphorylation. Such a hyperactivation can be achieved by expression of a constitutively active form of Ras (RasV12). We coexpressed GFP-Sec16 either with wild-type Ras or RasV12 linked to the ER (M1-RasV12). The ER version of RasV12 was previously shown to be a strong stimulator of the Raf–MEK–ERK pathway and cell growth (Matallanas et al., 2006). Sec16 phosphorylation was more than twofold higher in cells expressing RasV12 than in cells expressing wild-type Ras (Fig. 9 D). In addition, RasV12-expressing cells had a higher number of ERESs (Fig. 9 E), thereby linking Sec16 phosphorylation to ERES number. We conclude that Sec16 is a new target of ERK2.

Discussion

Genetic and biochemical analyses over the past three decades have provided profound understanding of the machineries mediating bidirectional ER–Golgi trafficking (Rothman and Wieland, 1996; Bonifacino and Glick, 2004; Lee et al., 2004), and considerable knowledge is available on organelle shape and proteomics (Gilchrist et al., 2006; Gillingham and Munro, 2007; Cai et al., 2007). What has almost entirely been lacking is an understanding of high-order regulation of the secretory pathway by cellular signaling pathways. A recent study reported that arrival of a cargo wave in the Golgi activates Src family kinases (Pulvirenti et al., 2008). Although this is an example for an adaptive response, it does not address the regulation of the secretory pathway by signaling under basal conditions.

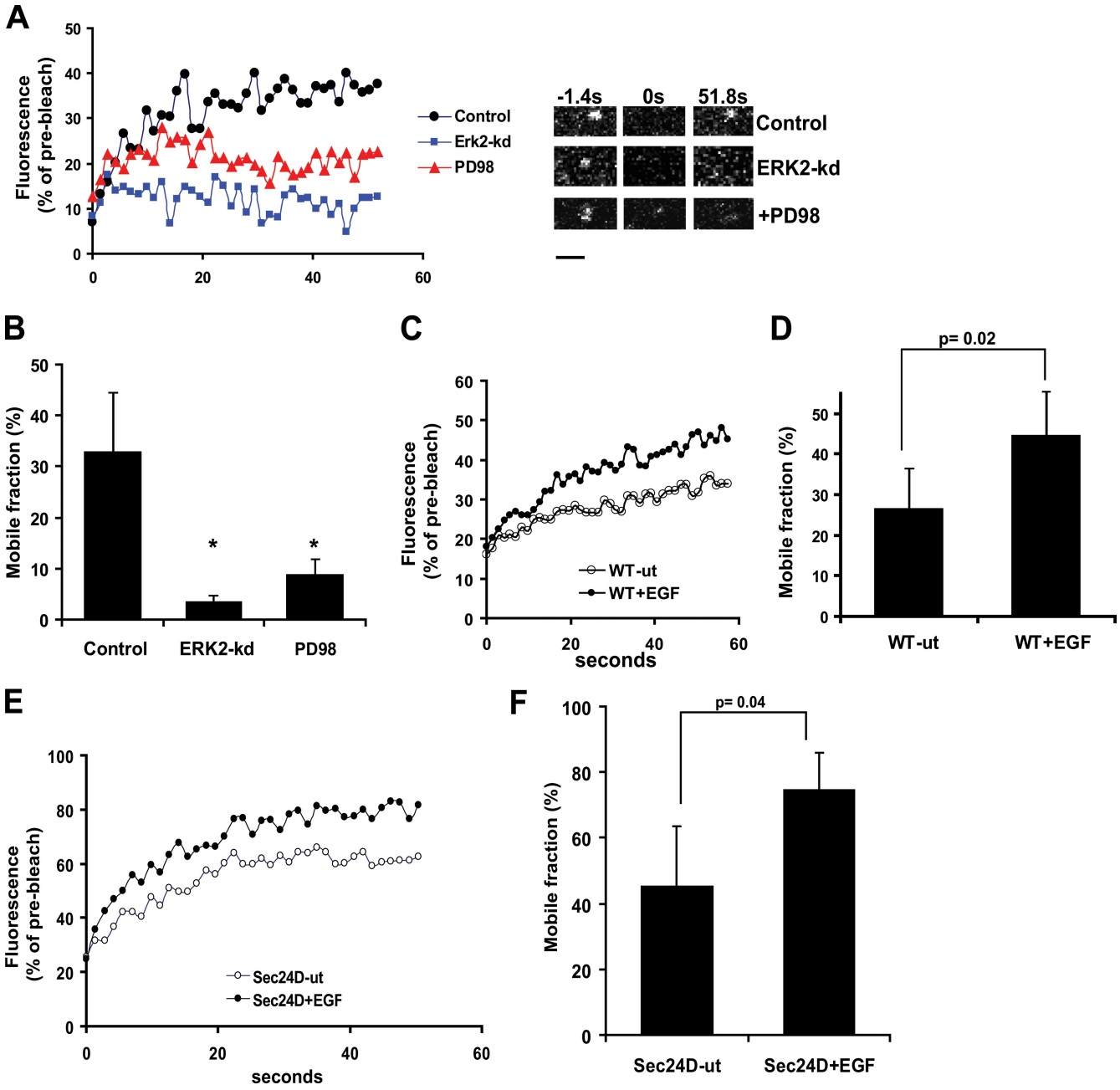

Figure 7. **Changes in Sec16 dynamics upon inhibition or activation of the MAPK pathway.** (A) Cells were transfected with control siRNA or siRNA to ERK2. After 48 h, cells were transfected with GFP-Sec16 cDNA, and 24 h later, FRAP analysis was performed. Of the two control siRNA–transfected cells, one dish was treated with solvent (control) and one with the MEK inhibitor PD98059 for 30 min before analysis. The right panel shows examples of bleached ERESs with indicated time points. (B) Quantification of mobile fractions from the curves in A (see Materials and methods). Asterisks indicate statistically significant differences (means ± SD; three independent experiments; *, $P < 0.01$; unpaired *t* test). (C) HeLa cells expressing GFP-Sec16 were serum starved for 8 h before the FRAP experiment (WT-ut). Afterward, cells were treated with EGF for 10 min, and further FRAP curves were recorded from the same dish (WT+EGF). (D) Quantification of mobile fractions from the curves in C (see Materials and methods; means ± SD; three independent experiments, four curves each; paired *t* test). (E) HeLa cells expressing YFP-Sec24D were serum starved for 8 h before the FRAP experiment (Sec24D-ut). Afterward, cells were treated with EGF for 10 min, and additional FRAP curves were recorded from the same dish (Sec24D+EGF). (F) Quantification of mobile fractions from the curves in E (see Materials and methods; means ± SD; three independent experiments, four curves each; paired *t* test). Bar, 1 µm.

Our siRNA screen provides a global view of kinase/phosphatase signaling to the early secretory pathway. Our key findings are as follows: (a) at least 122 kinases and phosphatases control the organization and/or traffic of the ER–Golgi system; (b) the Raf–MEK–ERK pathway controls ERES formation, COPII vesicle budding, and ER to Golgi transport; and (c) the ERES protein Sec16 is a target of the ERK2 pathway. Hyperactivation of the MAPK pathway increases, and its inhibition decreases ERES number. The range within which the ERES number was regulated by the MAPK pathway was 50%. Because this number is based on knockdown and not knockout conditions, the actual range in the cell may be even bigger.

A full-genome screen for regulators of secretion in *Drosophila melanogaster* cells revealed 130 hits (Bard et al., 2006).

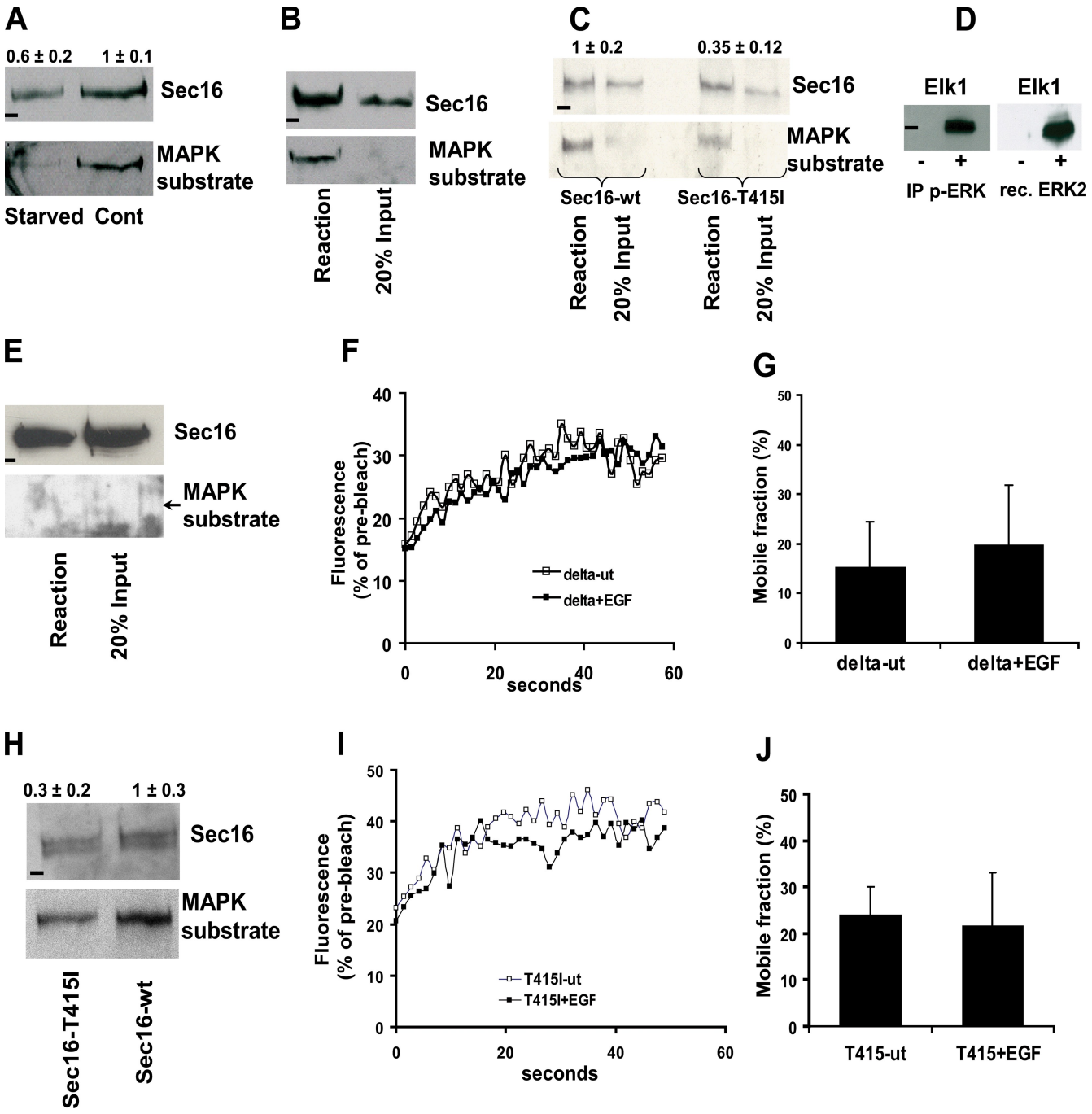

Figure 8. **Sec16 is a target of the MAPK pathway.** (A) Cells were transfected with GFP-Sec16 cDNA. After 8 h, medium was replaced by complete medium (Cont) or medium without serum (starved). Sec16 was immunoprecipitated with anti-GFP, subjected to SDS-PAGE, and immunoblotted with anti-Sec16 (top). The blot was stripped and reprobed with anti–MAPK substrate (bottom). The numbers above the blot indicate relative amounts determined by densitometric scanning. The intensity of the MAPK substrate band was normalized to the Sec16 band. To facilitate comparisons, the value of the control band was set to 1. Note that starvation reduces phosphorylation of Sec16 by 40% (means ± SD; three independent experiments; $P < 0.05$). (B) Cells were transfected with GFP-Sec16 and, after 8 h, serum starved. Sec16 was immunoprecipitated with anti-GFP. A parallel cell culture was treated with EGF. Active ERK was immunoprecipitated with agarose-coupled anti–phospho-ERK and incubated with the immunoprecipitated active ERK. Immunoprecipitated GFP-Sec16 and immunoprecipitated phospho-ERK were mixed, and the kinase reaction was performed for 30 min at 30°C (reaction). 50% of the reaction was separated by SDS-PAGE and immunoblotted with anti-Sec16 (top). The blot was stripped and reprobed with anti–MAPK substrate (bottom). (C) Cells were transfected with GFP-Sec16 cDNA (wild type [wt] or T415I). Immunoprecipitated Sec16 (anti-GFP) was coincubated with active ERK2 and ATP for 30 min at 30°C. 50% of the reaction was loaded, subjected to SDS-PAGE, and immunoblotted with anti-Sec16 (top). The blot was stripped and reprobed with anti–MAPK substrate antibody (bottom). The numbers above the blot indicate relative amounts determined by densitometric scanning. The intensity of the MAPK substrate band was normalized to the Sec16 band. To facilitate comparisons, the value of the control band was set to 1. Note that the mutation of T415I reduces the ability of ERK2 to phosphorylate Sec16 by at least 65% (means ± SD; three independent experiments). (D) Phosphorylation of purified GST-tagged Elk1 by immunoprecipitated phospho-ERK1/2 (IP p-ERK) as described in B or recombinant active ERK2 (rec. ERK2). The reaction was performed at 30°C for 30 min either with buffer (−) or with the kinase (+). (E) HeLa cells were transfected with a plasmid encoding GFP-Sec16 lacking the N-terminal 923 aa. Sec16 was immunoprecipitated with anti-GFP and incubated with active ERK2 and ATP for 30 min at 30°C. Samples were subjected to SDS-PAGE and immunoblotting with anti-Sec16 (top). The blot was stripped and reprobed with anti–MAPK substrate antibody (bottom). The arrow indicates the position

The comparatively high number of kinases/phosphatases (122) affecting the early secretory pathway in our screen appears surprising at first sight. This difference is largely caused by the fact that the *Drosophila* screen monitored secretion of a soluble protein rather than morphological changes of the secretory pathway. Most of our kinase hits are specific to the early secretory pathway as they overlap with only 12% of hits from a screen for kinases affecting clathrin- and caveolae-mediated endocytosis (Table S2; Pelkmans et al., 2005).

Signaling involved in mitotic Golgi fragmentation has been elucidated in quite some detail (Colanzi et al., 2003). In contrast, the role of signaling in Golgi structure regulation during interphase remains largely unknown. Mitotic Golgi fragmentation depends on signaling via MEK and ERK (Shaul and Seger, 2006; Feinstein and Linstedt, 2008). A recent study shows that MEK to ERK signaling to the Golgi does not involve the classical MEK1/2 to ERK1/2 route. Mitotic Golgi fragmentation was mediated by a splice variant of MEK1, MEK1b, which activates a splice variant of ERK1 termed ERK1c (Shaul et al., 2009). Consistent with this observation, we have no indication for a role of ERK signaling to the Golgi in interphase cells, as treatment with EGF did not fragment the Golgi (unpublished data).

An RNAi screen was recently performed to find regulators of cell migration (Simpson et al., 2008). The library targeted 1,081 human genes encoding phosphatases, kinases, and proteins predicted to influence cell migration and adhesion. The screen identified 79 high and medium confidence genes that impaired cell migration. Because we propose that our Golgi-class hits regulate cell migration, we expected to find a considerable overlap. However, this was not the case. The only gene common to both studies is CDK4, which we found to inhibit Golgi orientation in the wound-healing assay (Fig. 4 B). However, the screen of Simpson et al. (2008) failed to retrieve kinases known to regulate cell migration such as MAPK9, -10, and -14, which appeared as Golgi-class hits in our screen. These hits indicate that our collection of kinases/phosphatases required for maintaining Golgi structure is a promising resource for future studies on Golgi ribbon maintenance and its role in directional cell migration as well as in the cellular processes shown in Fig. 3 B.

How growth factors signal to the secretory pathway has been unknown. In this study, we show that growth factors signal to ERESs via the Raf–MEK–ERK pathway in an ERK2-dependent manner. Besides ERK2, upstream activators and positive modulators of ERK2, including Raf1, A-Raf, CNK1, MEKK1, and the EGF receptor, were retrieved as ER-class hits. We did not find MEK1 and -2 in our screen, most likely because of redundant signaling at this level of the MAPK pathway. The human kinome contains 20 kinases at the level of MAPK kinase kinase (MAP3K1–14, Raf1, A-Raf, B-Raf, and TAO kinases 1–3) and 14 at the level of MAPK (MAPK1 and MAPK3–15). However, there are only seven kinases at the level of MAPK kinase (MAP2K1–7). This fact points to a high degree of redundancy between different MAPK kinases. MEK1 and -2 share 85% sequence identity. Their abilities to phosphorylate ERK1 and -2 are similar, and individual deletion of MEK1 or -2 in skin fibroblasts does not reduce the amount of active ERK1/2 (Scholl et al., 2007). To the contrary, a single deletion of MEK1 seems to increase the level of active ERK1/2 (Catalanotti et al., 2009). In view of these considerations, it is not surprising that we did not hit MEK1/2.

We provide evidence that the effect of ERK2 on ERESs is mediated by Sec16, a major regulator of ERES homeostasis. Sec16 was directly phosphorylated by immunoprecipitated ERK and by recombinant active ERK2, most likely on T415. This residue was found to be phosphorylated in vivo (Olsen et al., 2006). Expression of a constitutively active Ras version resulted in an increase in Sec16 phosphorylation and in an increase in ERES number. This finding links the phosphorylation of Sec16 to the number of ERESs. Our combined data suggest the signaling model illustrated in Fig. 10. Although important, ERK2 may not be the only regulator of Sec16. According to the Phosida database (http://www.phosida.com), there are 49 sites in Sec16 that are phosphorylated, but their functional relevance is unknown. Moreover, it is worth noting that the ERES localization of Sec16 is determined by a sequence of basic amino acids in the central conserved domain of the protein (Ivan et al., 2008). The role of ERK2 is to modulate this localization in a dynamic way. Because growth factor signaling increases protein synthesis, we speculate that ERK2 adjusts ERESs to cope with this condition. In addition, environmental changes (e.g., nutrients and mitogens) can be sensed and this information transmitted via the MAPK pathway to instruct ERESs to change the rate of cargo flux.

Alterations of the MAPK pathway may indirectly affect ERES number by changing the translation rate and thereby cargo load. Although we cannot entirely rule out this possibility, the following considerations argue for a direct effect. First, pharmacological inhibition of the MAPK pathway (by PD98054 for 30 min) reduced ER to Golgi transport of α1-antitrypsin

where a band would be expected in case of corresponding phosphorylation. (F) HeLa cells expressing GFP-tagged truncation mutant of Sec16 lacking the N-terminal 923 aa (delta) were serum starved for 8 h before the FRAP experiment (delta-ut). Afterward, cells were treated with EGF for 10 min, and further FRAP curves were recorded from the same dish (delta+EGF). (G) Quantification of the mobile fractions from the curves in F (see Materials and methods; means ± SD; three independent experiments). (H) Cells were transfected with GFP-Sec16 cDNA (wild type [wt] or T415I). Sec16 was immunoprecipitated with anti-GFP, subjected to SDS-PAGE, and immunoblotted with anti-Sec16 (top). The blot was stripped and reprobed with anti–MAPK substrate (bottom). The numbers above the blot indicate relative amounts determined by densitometric scanning. The intensity of the MAPK substrate band was normalized to the Sec16 band. To facilitate comparisons, the value of the control band was set to 1. Note that the T415I mutation reduces the phosphorylation of Sec16 down to 30% (means ± SD; four independent experiments). (I) HeLa cells expressing GFP-tagged Sec16-T415I were serum starved for 8 h before the FRAP experiment (T415I-ut). Thereafter, the cells were treated with EGF for 10 min, and additional FRAP curves were recorded from the same dish (T415I+EGF). (J) Quantification of the mobile fractions from the curves in I (see Materials and methods; means ± SD; three independent experiments). (A–E and H) Black lines on the blots indicate the position of the 250-kD (A–C), 50-kD (D), 150-kD (E), or 250-kD (H) molecular mass marker.

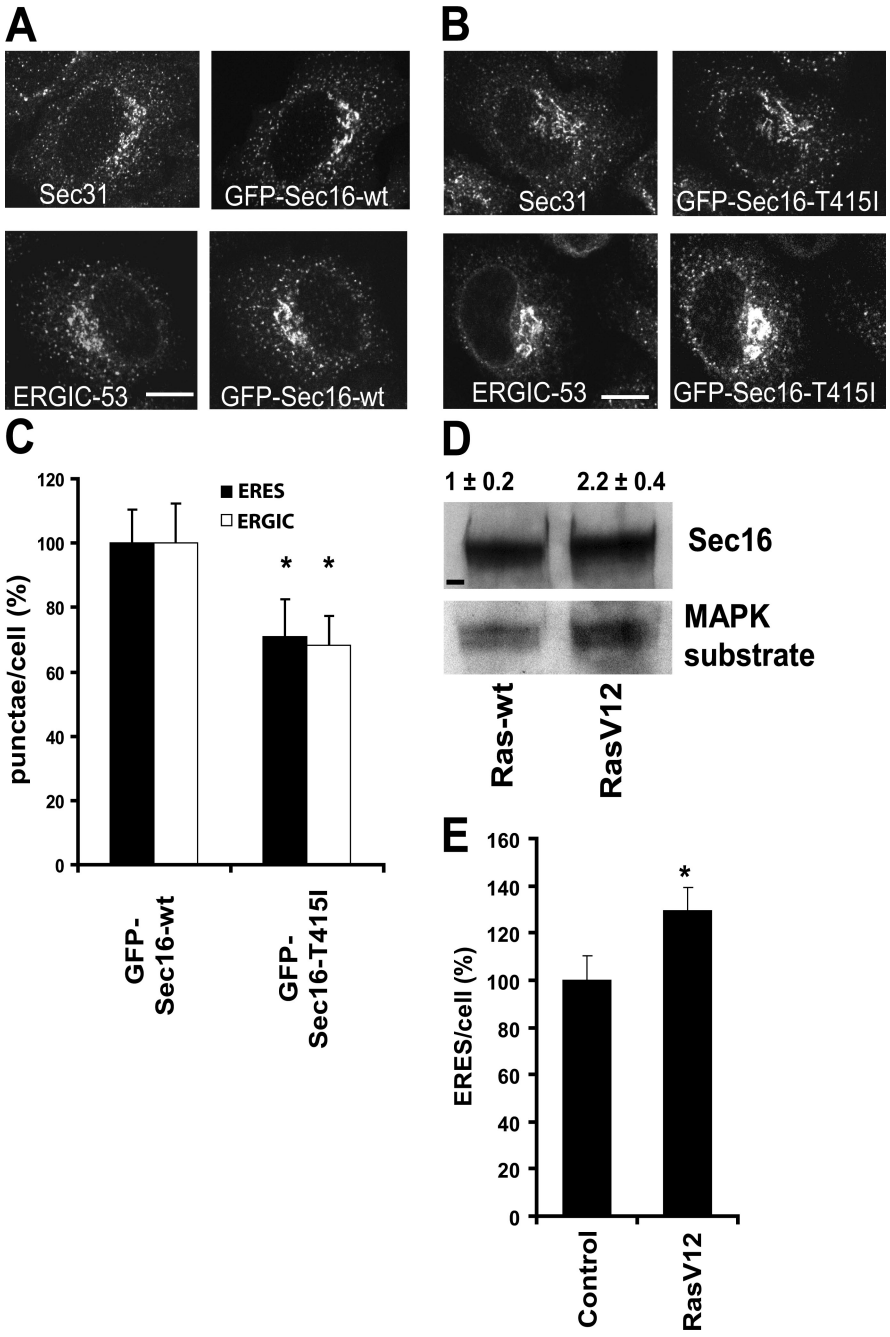

Figure 9. **Phosphorylation of Sec16 is linked to ERES number.** (A–C) Hells cells were transfected with cDNA encoding wild-type GFP-Sec16 (GFP–Sec16-wt; A) or GFP–Sec16-T415I (B), fixed 24 h later, and immunostained for Sec31 to label ERESs or ERGIC-53 to label the ERGIC. (C) The number of ERESs and peripheral ERGIC punctae was counted. The bar graph represents the number of punctae positive for Sec31 (ERES) or ERGIC-53 (ERGIC). The values determined in cells expressing GFP–Sec16-wt were set to 100% (means ± SD; three independent experiments; asterisks indicate statistically significant difference to GFP–Sec16-wt; *, $P < 0.05$; unpaired *t* test). (D) Cells were transfected with cDNA for GFP-Sec16 together with either wild-type H-Ras (Ras-wt) or M1–H-RasV12 (RasV12). Sec16 was immunoprecipitated with anti-GFP, subjected to SDS-PAGE, and immunoblotted with anti-Sec16 (top). The blot was stripped and reprobed with anti–MAPK substrate (bottom). The numbers above the blot indicate relative amounts determined by densitometric scanning. The intensity of the MAPK substrate band was normalized to the Sec16 band. To facilitate comparisons, the mean value of the samples transfected with wild-type Ras was set to one (mean ± SD; three independent experiments). The black line on the blot indicates the position of the 250-kD molecular mass marker. (E) Cells were transfected with cDNA for HA-tagged M1-RasV12. After 24 h, cells were fixed and costained for HA (RasV12) and Sec31. The bar graph shows ERESs/cell comparing cells expressing RasV12 or not (control; means ± SD; three independent experiments; asterisk indicates statistically significant difference; *, $P < 0.05$ from control; unpaired *t* test). Bars, 10 µm.

(Fig. 5 E). Second, ERK2 directly stimulated COPII vesicle budding in vitro (Fig. 6). Third, pharmacological inhibition of the MAPK pathway (by PD98054 for 30 min) altered Sec16 dynamics on ERESs (Fig. 7 A). Fourth, NF1 knockdown, which hyperactivates the Raf–MEK–ERK pathway, did not induce ER stress (unpublished data). Stress induction would be expected if the increase in ERES number was a result of cargo overload (Farhan et al., 2008).

Our discovery of a link between the MAPK pathway and ER export provides a framework for a better mechanistic understanding of diseases associated with alterations of secretion. A case in point is hypersecretion of immunoglobulins observed in autoimmune disorders. ERK1 knockout mice are more prone to autoimmunity and have 10-fold higher plasma immunoglobulin levels. They display increased levels of basal ERK2 phosphorylation and thus activity (Agrawal et al., 2006). We speculate that stimulation of immunoglobulin secretion is, at least in part, caused by augmented ERK2 levels. Another example is the antibody-mediated autoimmune disease systemic lupus erythematosus (SLE). Both in a mouse model of SLE and in a subset of SLE patients, a point mutation in the receptor leukocyte Tyr kinase (LTK) was identified that renders this enzyme hyperactive (Li et al., 2004). LTK is one of our ER-class hits, and its silencing strongly reduced the number of ERESs and ER to Golgi transport (unpublished data). It is tempting to speculate that LTK has a direct regulatory role in immunoglobulin secretion.

In conclusion, our study provides not only a resource of signaling molecules involved in the regulation of morphology

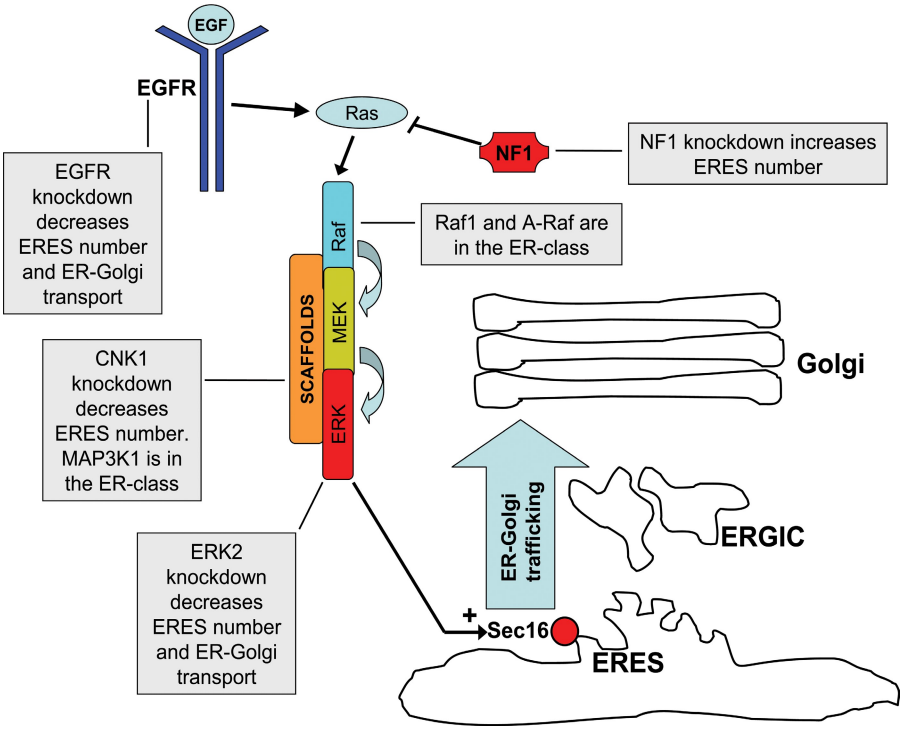

Figure 10. **Model of the pathway signaling to ERESs.** EGFR, EGF receptor.

and function of the secretory pathway but also uncovers growth factor signaling to ERESs via ERK2. The latter finding expands the already complex repertoire of cellular functions of ERKs and may have implications for understanding various disease states involving the MAPK pathway, including autoimmunity, cancer, and RAS/MAPK syndromes.

Materials and methods

High-throughput siRNA screening

The procedure was performed essentially as described previously (Pelkmans et al., 2005). In brief, HeLa cells (1,000 per well) were seeded into 384-well plates and transfected 24 h later with 20 µM siRNA complexed with INTERFERin (Polyplus Transfection) as delivery agent. After 48 h, cells were fixed and labeled with 3.7% paraformaldehyde. Images were acquired using the Opera automated spinning disk confocal microscope (PerkinElmer).

FRAP microscopy

HeLa cells expressing GFP-tagged Sec16 (Addgene) or YFP-tagged Sec24D (gift from R. Pepperkok, European Molecular Biology Laboratory, Heidelberg, Germany) were cultured on glass coverslips, transferred to imaging medium 1 (Ham's F12 supplemented with 20 mM Hepes, pH 7.4) in a Ludin chamber (Life Imaging Services GmbH), and imaged with a 63× oil objective on a microscope (SP5; Leica) at room temperature. All FRAP experiments were performed by bleaching individual ERESs. A prebleaching scan was performed, and the area of interest was subsequently bleached at full laser power for 1.4 s. Pictures were taken every 1.4 s for 56 s, converted to TIF files, and analyzed using ImageJ 1.4g (National Institutes of Health). Fluorescence values of the region of interest were normalized to prebleaching values. The mobile fraction was calculated according to Reits and Neefjes (2001) following the equation $R = (F_\infty - F_0)/(F_i - F_0)$, where F_∞ is fluorescence in the bleached region after recovery, F_i is the fluorescence in the bleached region before bleaching, and F_0 is the fluorescence in the bleached region directly after bleaching.

Cell culture and transfection

HeLa cells were cultured in DME containing 10% FBS and antibiotics. For gene silencing, cells cultured in 6-well plates were transfected with 5 nM siRNA using HiPerFect (QIAGEN) and typically analyzed after 72 h. cDNA transfection was performed using FuGene6 (Roche) 24 h before analysis.

Antibodies and immunofluorescence microscopy

Monoclonal antibodies to ERGIC-53 (Schweizer et al., 1988), Sec31 (BD), and GFP (Roche) were used. Rabbit antibodies to giantin (gift of A. Linstedt, Carnegie Mellon University, Pittsburgh, PA), Sec24A and -B (gift of J.-P. Paccaud, Drugs for Neglected Diseases Initiative, Geneva, Switzerland), Sec31 (gift of F. Gorelick, Yale University, New Haven, CT; Shugrue et al., 1999), ERK1/2, phosphorylated ERK1/2, MAPK substrate, PKC substrate (Cell Signaling Technology), Sec16 (Iinuma et al. 2007), Sec24D (Wendeler et al., 2007), and XBP1s (BioLegend) were also used. FITC–Con A was obtained from Invitrogen. HeLa cells were fixed with 3% paraformaldehyde, pH 7.4, for 30 min at room temperature, permeabilized for 4 min with PBS supplemented with 20 mM Gly, 0.2% Triton X-100, and 3% bovine serum albumin, and stained with antibodies. Images were acquired with a confocal microscope (SPE; Leica) using a 40× oil objective. For counting peripheral ERGIC clusters and ERESs, images were acquired with an additional 1.5 magnification in one confocal plane with a thickness of typically 210 nm. The raw images were converted to TIF files and analyzed using ImagePro Plus software (Media Cybernetics). Anti-Sec31–labeled ERESs were defined as bright objects in the top 80% of the intensity scale with a diameter of >1.5 pixels. This evaluation allows exclusion of objects that are too dim and too small and thereby avoids counting false objects that may occur as the result of the pixelization of images. Alternatively, ERESs were counted using ImageJ. Here, all circular objects were analyzed. The threshold was set individually for every image to assure that only true ERESs were counted. Both methods produced very similar results. For the counting of ERESs, 25–84 cells were evaluated per condition, and three independent experiments were performed. In experiments dealing with transfected GFP-Sec16, we only chose moderately expressing cells. Here, we used 10–19 cells per condition in three independent experiments.

Pulse-chase experiments

HeLa cells (2×10^5 in 2.5-cm dishes) were transfected with 5 nM siRNA. Pulse-chase experiments were performed 72 h after transfection. Cells were incubated in Met-free DME (supplemented with Gln and dialyzed FBS) for 20 min and pulsed in medium containing [^{35}S]Met (100 µCi/dish) for 10 min. The medium was then replaced by complete DME containing 10 mM nonlabeled Met. Cells were lysed after different chase times and subjected to immunoprecipitation.

Vesicle budding assay

The following buffers were used: buffer E (50 mM Hepes-KOH, pH 7.2, 250 mM sorbitol, 70 mM KOAc, 5 mM EDTA, and 0.5 mM MgOAc), buffer F (10 mM Hepes-KOH, pH 7.2, 250 mM sorbitol, 10 mM KOAc,

and 1.5 mM MgOAc), and buffer G (20 mM Hepes-KOH, pH 7.2, 250 mM sorbitol, 140 mM KOAc, and 0.5 mM MgOAc). The method of Kim et al. (2005) was used and adapted as follows. The preparation of cytosol and microsomes was performed at 4°C. Cytosol was prepared from HeLa cells (six 10-cm dishes) that were knocked down for ERK2. Cells were scraped into 2 ml of buffer E and centrifuged at 500 *g* for 10 min. The cell pellet was resuspended in 50 µl per 10-cm dish of buffer E. Cells were passed through a 25-gauge syringe at least 30 times and centrifuged at 1,000 *g* for 10 min. The postnuclear supernatant was centrifuged at 100,000 *g* for 30 min. The supernatant was used as cytosol. It had a mean protein concentration of 2–2.5 mg/ml. For the preparation of microsomes, cells of three 10-cm dishes were scraped into 1 ml PBS and centrifuged at 500 *g* for 10 min. The pellet was resuspended in 400 µl of buffer F. Cells were passed through a 25-gauge syringe at least 30 times and centrifuged at 1,000 *g* for 10 min. The postnuclear supernatant was centrifuged at 6,000 *g* for 10 min. The pellet was resuspended in 400 µl of buffer G and recentrifuged at 6,000 *g* for 10 min at 4°C. The pellet was resuspended in 96 µl of buffer G. For a typical budding reaction, 30 µl of microsomes and 65 µl of cytosol were used. The reaction mixture contained 0.5 mM GTP (Sigma-Aldrich) and an ATP regeneration system (1 mM ATP, 25 mM creatine phosphate, and 0.3 mg/ml creatine kinase; Sigma-Aldrich). The reaction was performed for 30 min at 25°C or on ice (control). In the ERK2-containing reactions, 100 ng recombinant active ERK2 (activated by purifying from cells expressing constitutive active MEK1; Cell Signaling Technology) was added. The reaction was terminated by transferring the tubes to ice. Microsomes were collected by centrifugation at 16,000 *g* for 10 min. The supernatant was centrifuged at 100,000 *g* for 40 min to pellet the budded vesicles. Budding efficiency was calculated as $(V/M_{ERGIC\text{-}53} \times 100) - (V/M_{CLIMP63} \times 100)$. To show that the budding assay for ERGIC-53 is COPII dependent, we performed budding assays with cytosol immunodepleted for Sec24A and -B (Wendeler et al., 2007).

Immunoprecipitation

For each immunoprecipitation experiment with GFP-tagged Sec16, three 10-cm dishes (70% confluent cells) were used. Cells were transfected with GFP-tagged Sec16 cDNA. After 24 h, cells were lysed in 800 µl of immunoprecipitation buffer (50 mM Tris-HCl, pH 7.4, 150 mM NaCl, 2 mM $CaCl_2$, and 1% Triton X-100). The lysate was incubated on ice for 10 min and cleared by centrifugation at 16,000 *g* for 10 min at 4°C. To the cleared lysate, protein G–Sepharose was added to which anti-GFP antibody had been preadsorbed. This mixture was incubated overnight with gentle agitation at 4°C. On the next day, the beads were washed three times, and Sec16 was eluted by boiling in sample buffer. For the kinase assay, the beads were washed thrice with kinase buffer (Cell Signaling Technology) and finally resuspended in 30 µl of this buffer.

Mutagenesis of Sec16

The following primer pair was used (the mutated triplet is underlined and bold): Thr415Ile, 5′-CGTGTCCCAGCCCTCA**ATT**CCGAGCCCCCCG-3′ and 5′-CGGGGGGCTCGG**AAT**TGAGGGCTGGGACACG-3′. A two-step PCR mutagenesis method was used. Two PCR reactions were performed in parallel, each containing only one primer. A typical PCR mixture (50 µl volume) contained 1 µl DNA (50 ng final), 1 µl Pfu polymerase, 5 µl of 10× buffer, 4 µl of primer (0.8 µM final concentration), 4 µl dNTP mixture (0.2 µM final concentration), and 35 µl water. The first PCR reaction was performed for 10 cycles (60 s at 95°C, 90 s at 55°C, and 21 min at 68°C). 25 µl of each reaction was then pooled, and 0.7 µl Pfu polymerase was added. The second PCR reaction was performed for 18 cycles with the same conditions. PCR products were digested with DpnI for 3 h at 37°C and used to transform *Escherichia coli*. On the next day, colonies were picked and grown in 3-ml cultures overnight. 1 d later, plasmids were prepared using the GenElute Plasmid Miniprep kit (Sigma-Aldrich). All mutations were verified by sequencing.

Statistics

All data analysis was performed using Excel2003 (Microsoft). Error bars on all graphs are mean ± SD from three independent measurements, except where indicated otherwise in the figures. Statistical significance was calculated using the *t* test, and $P < 0.05$ was considered significant.

Bioinformatic analysis

Interaction networks were generated using the STRING database. Only interactions supported by biochemical evidence or databases (including Kyoto Encyclopedia of Genes and Genomes, Reactome, and Pathway Interactin Database) were considered. Anchored networks were created using the Cytoscape software (version 2.6.3; http://cytoscape.org/) using an algorithm described by Yosef et al. (2009). The following parameters were used when a BiNGO analysis (of *Homo sapiens* GO annotations) was performed: hypergeometric test, Benjamini-Hochberg false discovery rate correction (to correct for multiple testing), significance value 0.001, and GO biological processes. Each cluster was tested against the whole annotation.

Online supplemental material

Fig. S1 shows the distribution of ER-, mixed-, and Golgi-class hits in several signaling pathways. Fig. S2 shows the impact of NF1 or CNK1 knockdowns on ERK1/2 activation. Fig. S3 shows the effect of Sec24A+B depletion or ERK1 on budding of ERGIC-53. Table S1, included as an Excel file, contains a list of all kinases phosphatases that have been targeted and the ID numbers of the siRNAs that were used to target them. Table S2, included as an Excel file, contains a list of all 122 hits classified into ER-, mixed-, and Golgi-class hits and information about tubulin staining and the effect on the number of peripheral ERGIC punctae and cites evidence for the expression of the gene in HeLa cells. A zip file contains large PDF versions of the networks in Fig. 3 and their underlying data (which can be opened and visualized in Cytoscape). Online supplemental material is available at http://www.jcb.org/cgi/content/full/jcb.200912082/DC1.

We thank Benjamin Glick, Michael N. Hall, Ari Helenius, Jennifer Lippincott-Schwartz, Vivek Malhotra, Sean Munro, and James Rothman for comments; members of the Hauri group for their contributions; Randy Schekman for an important suggestion regarding the vesicle budding assay; Fred Gorelick, Jean-Pierre Paccaud, Adam Linstedt, Piero Crespo, Gerald Radziwill, Rainer Pepperkok, Melanie Cobb, Mark Philips, and Katsuko Tani for reagents; Nir Yosef and Eytan Ruppin for their help with analyzing the Golgi networks; and Claudia Moebius and Kerstin Korn for assistance in the screening process.

H. Farhan was supported by a Schrödinger Fellowship of the Austrian Science Foundation and a European Molecular Biology Organization long-term fellowship. This work was supported by the Swiss National Science Foundation and the Universität Basel.

Submitted: 14 December 2009
Accepted: 17 May 2010

References

Agrawal, A., S. Dillon, T.L. Denning, and B. Pulendran. 2006. ERK1-/- mice exhibit Th1 cell polarization and increased susceptibility to experimental autoimmune encephalomyelitis. *J. Immunol.* 176:5788–5796.

Appenzeller-Herzog, C., and H.P. Hauri. 2006. The ER-Golgi intermediate compartment (ERGIC): in search of its identity and function. *J. Cell Sci.* 119:2173–2183. doi:10.1242/jcs.03019

Bard, F., L. Casano, A. Mallabiabarrena, E. Wallace, K. Saito, H. Kitayama, G. Guizzunti, Y. Hu, F. Wendler, R. Dasgupta, et al. 2006. Functional genomics reveals genes involved in protein secretion and Golgi organization. *Nature*. 439:604–607. doi:10.1038/nature04377

Bejarano, E., M. Cabrera, L. Vega, J. Hidalgo, and A. Velasco. 2006. Golgi structural stability and biogenesis depend on associated PKA activity. *J. Cell Sci.* 119:3764–3775. doi:10.1242/jcs.03146

Ben-Tekaya, H., K. Miura, R. Pepperkok, and H.P. Hauri. 2005. Live imaging of bidirectional traffic from the ERGIC. *J. Cell Sci.* 118:357–367. doi:10.1242/jcs.01615

Bhattacharyya, D., and B.S. Glick. 2007. Two mammalian Sec16 homologues have nonredundant functions in endoplasmic reticulum (ER) export and transitional ER organization. *Mol. Biol. Cell.* 18:839–849. doi:10.1091/mbc.E06-08-0707

Blumental-Perry, A., C.J. Haney, K.M. Weixel, S.C. Watkins, O.A. Weisz, and M. Aridor. 2006. Phosphatidylinositol 4-phosphate formation at ER exit sites regulates ER export. *Dev. Cell.* 11:671–682. doi:10.1016/j.devcel.2006.09.001

Bonifacino, J.S., and B.S. Glick. 2004. The mechanisms of vesicle budding and fusion. *Cell*. 116:153–166. doi:10.1016/S0092-8674(03)01079-1

Burman, J.L., L. Bourbonniere, J. Philie, T. Stroh, S.Y. Dejgaard, J.F. Presley, and P.S. McPherson. 2008. Scyl1, mutated in a recessive form of spinocerebellar neurodegeneration, regulates COPI-mediated retrograde traffic. *J. Biol. Chem.* 283:22774–22786. doi:10.1074/jbc.M801869200

Cai, H., K. Reinisch, and S. Ferro-Novick. 2007. Coats, tethers, Rabs, and SNAREs work together to mediate the intracellular destination of a transport vesicle. *Dev. Cell*. 12:671–682. doi:10.1016/j.devcel.2007.04.005

Catalanotti, F., G. Reyes, V. Jesenberger, G. Galabova-Kovacs, R. de Matos Simoes, O. Carugo, and M. Baccarini. 2009. A Mek1-Mek2 heterodimer

determines the strength and duration of the Erk signal. *Nat. Struct. Mol. Biol.* 16:294–303. doi:10.1038/nsmb.1564

Colanzi, A., C. Suetterlin, and V. Malhotra. 2003. Cell-cycle-specific Golgi fragmentation: how and why? *Curr. Opin. Cell Biol.* 15:462–467. doi:10.1016/S0955-0674(03)00067-X

Farhan, H., M. Weiss, K. Tani, R.J. Kaufman, and H.P. Hauri. 2008. Adaptation of endoplasmic reticulum exit sites to acute and chronic increases in cargo load. *EMBO J.* 27:2043–2054. doi:10.1038/emboj.2008.136

Feinstein, T.N., and A.D. Linstedt. 2008. GRASP55 regulates Golgi ribbon formation. *Mol. Biol. Cell*. 19:2696–2707. doi:10.1091/mbc.E07-11-1200

Gilchrist, A., C.E. Au, J. Hiding, A.W. Bell, J. Fernandez-Rodriguez, S. Lesimple, H. Nagaya, L. Roy, S.J. Gosline, M. Hallett, et al. 2006. Quantitative proteomics analysis of the secretory pathway. *Cell*. 127:1265–1281. doi:10.1016/j.cell.2006.10.036

Gillingham, A.K., and S. Munro. 2007. The small G proteins of the Arf family and their regulators. *Annu. Rev. Cell Dev. Biol.* 23:579–611. doi:10.1146/annurev.cellbio.23.090506.123209

Huang, W., B.T. Sherman, and R.A. Lempicki. 2009. Systematic and integrative analysis of large gene lists using DAVID bioinformatics resources. *Nat. Protoc.* 4:44–57. doi:10.1038/nprot.2008.211

Iinuma, T., A. Shiga, K. Nakamoto, M.B. O'Brien, M. Aridor, N. Arimitsu, M. Tagaya, and K. Tani. 2007. Mammalian Sec16/p250 plays a role in membrane traffic from the endoplasmic reticulum. *J. Biol. Chem.* 282:17632–17639. doi:10.1074/jbc.M611237200

Ivan, V., G. de Voer, D. Xanthakis, K.M. Spoorendonk, V. Kondylis, and C. Rabouille. 2008. *Drosophila* Sec16 mediates the biogenesis of tER sites upstream of Sar1 through an arginine-rich motif. *Mol. Biol. Cell*. 19:4352–4365. doi:10.1091/mbc.E08-03-0246

Jensen, L.J., M. Kuhn, M. Stark, S. Chaffron, C. Creevey, J. Muller, T. Doerks, P. Julien, A. Roth, M. Simonovic, et al. 2009. STRING 8—a global view on proteins and their functional interactions in 630 organisms. *Nucleic Acids Res.* 37:D412–D416. doi:10.1093/nar/gkn760

Kapetanovich, L., C. Baughman, and T.H. Lee. 2005. Nm23H2 facilitates coat protein complex II assembly and endoplasmic reticulum export in mammalian cells. *Mol. Biol. Cell*. 16:835–848. doi:10.1091/mbc.E04-09-0785

Karandikar, M., S. Xu, and M.H. Cobb. 2000. MEKK1 binds raf-1 and the ERK2 cascade components. *J. Biol. Chem.* 275:40120–40127. doi:10.1074/jbc.M005926200

Kim, J., S. Hamamoto, M. Ravazzola, L. Orci, and R. Schekman. 2005. Uncoupled packaging of amyloid precursor protein and presenilin 1 into coat protein complex II vesicles. *J. Biol. Chem.* 280:7758–7768. doi:10.1074/jbc.M411091200

Klumperman, J., A. Schweizer, H. Clausen, B.L. Tang, W. Hong, V. Oorschot, and H.P. Hauri. 1998. The recycling pathway of protein ERGIC-53 and dynamics of the ER-Golgi intermediate compartment. *J. Cell Sci.* 111:3411–3425.

Kolch, W. 2005. Coordinating ERK/MAPK signalling through scaffolds and inhibitors. *Nat. Rev. Mol. Cell Biol.* 6:827–837. doi:10.1038/nrm1743

Lee, M.C., E.A. Miller, J. Goldberg, L. Orci, and R. Schekman. 2004. Bi-directional protein transport between the ER and Golgi. *Annu. Rev. Cell Dev. Biol.* 20:87–123. doi:10.1146/annurev.cellbio.20.010403.105307

Letourneur, F., E.C. Gaynor, S. Hennecke, C. Démollière, R. Duden, S.D. Emr, H. Riezman, and P. Cosson. 1994. Coatomer is essential for retrieval of dilysine-tagged proteins to the endoplasmic reticulum. *Cell*. 79:1199–1207. doi:10.1016/0092-8674(94)90011-6

Li, N., K. Nakamura, Y. Jiang, H. Tsurui, S. Matsuoka, M. Abe, M. Ohtsuji, H. Nishimura, K. Kato, T. Kawai, et al. 2004. Gain-of-function polymorphism in mouse and human Ltk: implications for the pathogenesis of systemic lupus erythematosus. *Hum. Mol. Genet.* 13:171–179. doi:10.1093/hmg/ddh020

MacKeigan, J.P., L.O. Murphy, and J. Blenis. 2005. Sensitized RNAi screen of human kinases and phosphatases identifies new regulators of apoptosis and chemoresistance. *Nat. Cell Biol.* 7:591–600. doi:10.1038/ncb1258

Matallanas, D., V. Sanz-Moreno, I. Arozarena, F. Calvo, L. Agudo-Ibáñez, E. Santos, M.T. Berciano, and P. Crespo. 2006. Distinct utilization of effectors and biological outcomes resulting from site-specific Ras activation: Ras functions in lipid rafts and Golgi complex are dispensable for proliferation and transformation. *Mol. Cell. Biol.* 26:100–116. doi:10.1128/MCB.26.1.100-116.2006

Olsen, J.V., B. Blagoev, F. Gnad, B. Macek, C. Kumar, P. Mortensen, and M. Mann. 2006. Global, in vivo, and site-specific phosphorylation dynamics in signaling networks. *Cell*. 127:635–648. doi:10.1016/j.cell.2006.09.026

Orci, L., M. Ravazzola, P. Meda, C. Holcomb, H.P. Moore, L. Hicke, and R. Schekman. 1991. Mammalian Sec23p homologue is restricted to the endoplasmic reticulum transitional cytoplasm. *Proc. Natl. Acad. Sci. USA*. 88:8611–8615. doi:10.1073/pnas.88.19.8611

Palmer, K.J., J.E. Konkel, and D.J. Stephens. 2005. PCTAIRE protein kinases interact directly with the COPII complex and modulate secretory cargo transport. *J. Cell Sci.* 118:3839–3847. doi:10.1242/jcs.02496

Pelkmans, L., E. Fava, H. Grabner, M. Hannus, B. Habermann, E. Krausz, and M. Zerial. 2005. Genome-wide analysis of human kinases in clathrin- and caveolae/raft-mediated endocytosis. *Nature*. 436:78–86. doi:10.1038/nature03571

Preisinger, C., B. Short, V. De Corte, E. Bruyneel, A. Haas, R. Kopajtich, J. Gettemans, and F.A. Barr. 2004. YSK1 is activated by the Golgi matrix protein GM130 and plays a role in cell migration through its substrate 14-3-3ζ. *J. Cell Biol.* 164:1009–1020. doi:10.1083/jcb.200310061

Pulvirenti, T., M. Giannotta, M. Capestrano, M. Capitani, A. Pisanu, R.S. Polishchuk, E. San Pietro, G.V. Beznoussenko, A.A. Mironov, G. Turacchio, et al. 2008. A traffic-activated Golgi-based signalling circuit coordinates the secretory pathway. *Nat. Cell Biol.* 10:912–922. doi:10.1038/ncb1751

Reits, E.A., and J.J. Neefjes. 2001. From fixed to FRAP: measuring protein mobility and activity in living cells. *Nat. Cell Biol.* 3:E145–E147. doi:10.1038/35078615

Rivero, S., J. Cardenas, M. Bornens, and R.M. Rios. 2009. Microtubule nucleation at the cis-side of the Golgi apparatus requires AKAP450 and GM130. *EMBO J.* 28:1016–1028. doi:10.1038/emboj.2009.47

Rothman, J.E., and F.T. Wieland. 1996. Protein sorting by transport vesicles. *Science*. 272:227–234. doi:10.1126/science.272.5259.227

Scholl, F.A., P.A. Dumesic, D.I. Barragan, K. Harada, V. Bissonauth, J. Charron, and P.A. Khavari. 2007. Mek1/2 MAPK kinases are essential for Mammalian development, homeostasis, and Raf-induced hyperplasia. *Dev. Cell*. 12:615–629. doi:10.1016/j.devcel.2007.03.009

Schweizer, A., J.A. Fransen, T. Bächi, L. Ginsel, and H.P. Hauri. 1988. Identification, by a monoclonal antibody, of a 53-kD protein associated with a tubulo-vesicular compartment at the cis-side of the Golgi apparatus. *J. Cell Biol.* 107:1643–1653. doi:10.1083/jcb.107.5.1643

Shaul, Y.D., and R. Seger. 2006. ERK1c regulates Golgi fragmentation during mitosis. *J. Cell Biol.* 172:885–897. doi:10.1083/jcb.200509063

Shaul, Y.D., G. Gibor, A. Plotnikov, and R. Seger. 2009. Specific phosphorylation and activation of ERK1c by MEK1b: a unique route in the ERK cascade. *Genes Dev.* 23:1779–1790. doi:10.1101/gad.523909

Shugrue, C.A., E.R. Kolen, H. Peters, A. Czernik, C. Kaiser, L. Matovcik, A.L. Hubbard, and F. Gorelick. 1999. Identification of the putative mammalian orthologue of Sec31P, a component of the COPII coat. *J. Cell Sci.* 112:4547–4556.

Simpson, K.J., L.M. Selfors, J. Bui, A. Reynolds, D. Leake, A. Khvorova, and J.S. Brugge. 2008. Identification of genes that regulate epithelial cell migration using an siRNA screening approach. *Nat. Cell Biol.* 10:1027–1038. doi:10.1038/ncb1762

Supek, F., D.T. Madden, S. Hamamoto, L. Orci, and R. Schekman. 2002. Sec16p potentiates the action of COPII proteins to bud transport vesicles. *J. Cell Biol.* 158:1029–1038. doi:10.1083/jcb.200207053

Watson, P., A.K. Townley, P. Koka, K.J. Palmer, and D.J. Stephens. 2006. Sec16 defines endoplasmic reticulum exit sites and is required for secretory cargo export in mammalian cells. *Traffic*. 7:1678–1687. doi:10.1111/j.1600-0854.2006.00493.x

Wendeler, M.W., J.P. Paccaud, and H.P. Hauri. 2007. Role of Sec24 isoforms in selective export of membrane proteins from the endoplasmic reticulum. *EMBO Rep.* 8:258–264. doi:10.1038/sj.embor.7400893

Yadav, S., S. Puri, and A.D. Linstedt. 2009. A primary role for Golgi positioning in directed secretion, cell polarity, and wound healing. *Mol. Biol. Cell*. 20:1728–1736. doi:10.1091/mbc.E08-10-1077

Yosef, N., L. Ungar, E. Zalckvar, A. Kimchi, M. Kupiec, E. Ruppin, and R. Sharan. 2009. Toward accurate reconstruction of functional protein networks. *Mol. Syst. Biol.* 5:248. doi:10.1038/msb.2009.3

Zeuschner, D., W.J. Geerts, E. van Donselaar, B.M. Humbel, J.W. Slot, A.J. Koster, and J. Klumperman. 2006. Immuno-electron tomography of ER exit sites reveals the existence of free COPII-coated transport carriers. *Nat. Cell Biol.* 8:377–383. doi:10.1038/ncb1371